# Optimization of a Geometry for Single Measurement Air Kerma Strength Calibration Using Monte Carlo Simulations

_____

A Major Qualifying Project Report

Submitted to the Faculty of the

WORCESTER POLYTECHNIC INSTITUTE

in partial fulfillment of the requirements for the

Degree of Bachelor of Science


_____

By

Erika Kollitz



_____

Prof. David Medich, Ph.D., Major Advisor


_____

Prof. Robert Dempski, Ph.D., Co-Advisor

# Abstract

It is important to accurately characterize high dose rate (HDR) brachytherapy sources before use in cancer treatment. One of the standard ways to describe a source is the air kerma strength, which is measured using a seven-distance technique. However, this current method introduces a lot of uncertainty through photon attenuation, photon scatter, and data regression. MCNP was used to model and simulate a potential geometry for which only a single measurement in a vacuum would be required to more accurately measure air kerma. These simulations tested different radioisotopes, wall materials, and geometry sizes with the goal of minimizing scatter. The final optimized simulation will be used as a baseline for a physical construction that WPI can use to calibrate HDR brachytherapy sources.

# Table of Contents

# 1 Introduction

The average American has approximately a 40% chance of being diagnosed with cancer according to the most current data from the National Cancer Institute[1]. Of those diagnosed, one in five will die from the disease. In fact, the CDC ranks cancer of all kinds as the second leading cause of death in the United States behind heart disease[2]. The frequency and proliferation of cancer incidence in the US has prompted researchers to continue to press for safer and more efficient cancer treatments.

Popular treatments for cancer include surgery, chemotherapy, and radiation therapy. These therapies are often used in conjunction with each other, for example some types of chemotherapy can make the tumor cells more sensitive to the radiation therapy. Radiation therapy works by exposing the tumor to carefully calculated amounts of energy, leading to double strand breaks in the DNA of the cancerous cells and subsequent cell death. Therapy can be delivered in one of two ways, externally using directed beam therapy, and internally using implantable radioactive sources. This second type of radiation therapy using internally positioned sources is called brachytherapy. Brachytherapy with high levels of precision to deliver dose directly to the tumor while minimizing the exposure to healthy tissue.

In order to safely and efficiently devise a brachytherapy treatment plan, the exact characteristics of the sources (called seeds) need to be known. The better the sources are known, the more optimized the treatment plan and the lower the inherent risk. Brachytherapy seeds are manufactured to have specified characteristics, however it is possible for any two given seeds in a batch of Low Dose Rate seeds to differ in output by up to 11% [3]. This has lead the American Association of Physicists in Medicine (AAPM) to delegate to the medical physicists the responsibility of calibrating their sources before they are used for therapy so that any treatment plan is made with the correct and most accurate information. One characteristic commonly used to describe brachytherapy seeds is the air kerma strength.

Air kerma is the kinetic energy released in air due to incoming ionizing radiation and is measured in units of Gy (Joule/kg). It is used as a calibration standard for brachytherapy sources because it approximates absorbed dose while also being easier to measure. The most commonly used method of air kerma strength measurement is the seven-distance test. This method works by measuring the charge created in air due to a radioactive source at seven distances from the source[4]. The source needs to be measured seven different times at seven different positions in order to mathematically correct for error due to scatter and attenuation in the air between the source and detector, as well as the error inherent in positioning the detector[5]. In addition to this, the seven-distance apparatus must be very precise in order to accurately characterize the source.

The goal of this project is to design a possible geometry for single measurement air kerma strength calibration that minimizes scatter. Using computer simulation, the geometry was tested using different wall materials, different radioisotope point sources, and different sizes in order to optimize the system. The final geometry blueprint will be used as a basis to construct a physical version, which WPI can use in the future to efficiently calibrate brachytherapy sources.

# 2    Background

This project involves a great deal of background knowledge, such as the basics of radiation physics, radiation therapy, DNA interactions, and computer simulation. This section will discuss each of the topics required to understand the process of developing this project and its significance to radiation therapy application.

## 2.1    Radiation

Radiation is the emission and transmission of energetic particles or waves from a given source. There are many different types of radiation, each with their own properties and applications. Of particular interest is the radiation's ability to deposit energy into a material, as these processes can produce noticeable changes in that material whether it is causing biological damage or being used to produce energy. This section deals with the classification of different types of radiation as well as the properties and energy deposition processes of said radiation.

### 2.1.1  Radioisotopes

A nucleus is defined by the number of protons and neutrons contained within it. Those conditions define individual nuclides. If the nuclides all have the same number of protons, i.e. they are the same element, then they are called isotopes. Similarly, if the nuclides have the same number of neutrons they are called isotones, and if they have the same number of nucleons (they have the same atomic mass) they are called isobars.

Nuclides have varying levels of stability depending on their neutron/proton ratio. When the ratio is 1, indicating that there is an equal number of both nucleons, the isotope is generally stable, especially for elements of smaller Z. However, when there are an unequal number of protons and neutrons, the nuclide can emit radiation in order to stabilize themselves. Those nuclides that do emit radiation are called radioisotopes.

Included below in Figure 1 is the Table of Nuclides which shows the relative stability of all potential nuclides. The x axis describes the number of protons in the nucleus and the y axis is the number of neutrons. Each square is colored according to its stability, with the dark red nuclides being more stable and the blue-white nuclides being less stable. As the number of protons increases, the neutron-proton ratio of a perfectly stable nuclide also increases, such that a one to one ratio is no longer the most stable.
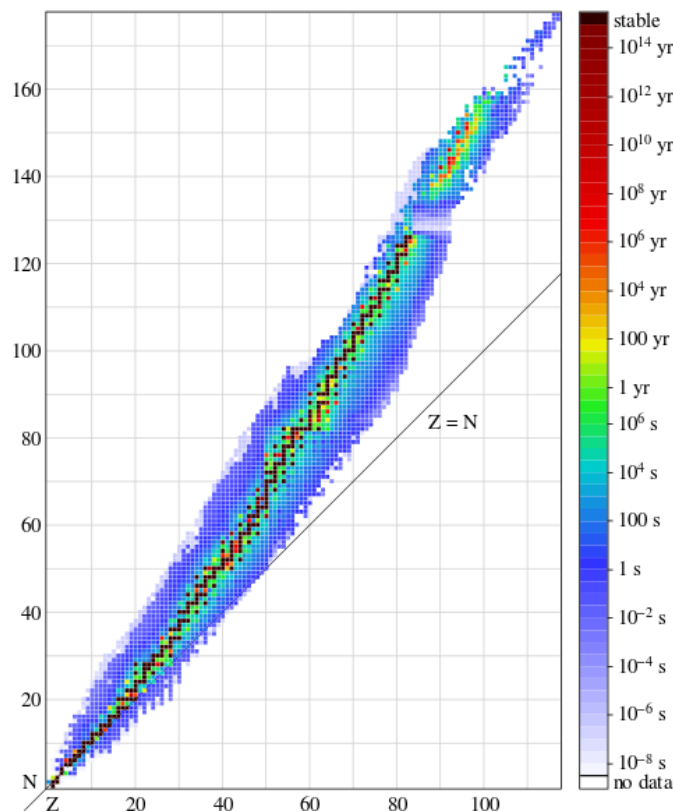
**Figure 1:** Table of Nuclides.[1]

### 2.1.2  Types of Radiation

Radiation can be classified based on the amount of energy it carries and by its physical characteristics. It is important to distinguish radiation based on energy because it easily informs as to its ability to interact with matter. Radiation which carries enough energy to free an electron from an atom is called "ionizing radiation". Any other radiation which cannot ionize an atom is called "non-ionizing radiation". Ionizing radiation is the more dangerous of the two, as the ability to liberate electrons from atoms means that it is capable of breaking the chemical bonds within organic material.

Aside from the distinction between ionizing and non-ionizing, radiation can also be separated based on the physical forms it can manifest as. The three main types of radiations are alpha, beta, and gamma. These types describe in what form energy is released from the radioisotope, but doesn't give any explicit information about the energy of the emissions. Each of these types have unique properties which lend them to differing applications.

Alpha radiation (α) describes the emission of a Helium nucleus from a larger atom. The alpha particle consists of two protons bound together with two neutrons, and tends to have a lower energy. In addition to this, it is relatively easy to shield against alpha radiation due to the coulombic forces caused by the positive charge on the two protons. In fact, alpha radiation can be stopped by something as thin and flimsy as a piece of paper.

---

[1] By BenRG (Own work) [Public domain], via Wikimedia Commons

Beta radiation (β) is the emission of either an electron or positron from the radioisotope. When the emitted particle is an electron it is called beta minus decay, and leaves the atom with a more positive charge. Conversely, an emission of a positron is a beta plus decay, and leaves the atom with a more negative charge. Beta decay results in the emission of only one nucleon as compared to alpha radiation's four, which means that it is can penetrate heavier and thicker barriers than alpha particles can.

Finally, gamma radiation (γ) is the release of a photon and tends to have a relatively high energy. Gamma radiation does not affect the neutron/proton ratio, but it does increase the stability of the atom by reducing its overall energy, and usually occurs when the atom is in an excited state. X-rays are identical to gamma rays, the difference between the two lies in how they are created. Where gamma rays are produced from a decay of an excited nucleus, x-rays are produced by either the collisions of electrons with a material (called Bremsstrahlung radiation and shown in Figure 2), or by the de-excitation of orbital electrons[6]. Since these radiation decays are not at all impeded by Coulomb forces, x and gamma rays can penetrate much farther even than beta particles.
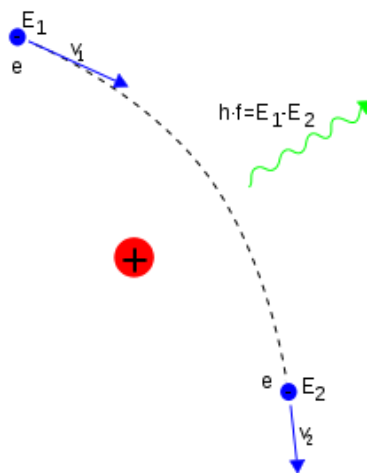


**Figure 2:** Bremsstrahlung Radiation[2]

There is another type of radiation which is not as common, but does occur called electron capture decay (ε) where an electron is absorbed into the nucleus, which then emits a neutrino. In the course of this reaction, a proton is converted into a neutron, which lowers the overall charge of the nucleus. In addition to this, because this process changes the number of protons, the element and nuclide of the atom changes as well, lowering its Z value. This can potentially lead to the release of a gamma ray since the new nuclide could have a ground state low enough to incite a further radiation event.

### 2.1.3  Radioactive Quantities

A couple of different properties of radioisotopes are worth noting. The first is half-life (τ), which describes the time that it takes for half of a sample of a particular radioactive element to decay. This property is specific to each nuclide, and is often used as a way to predict the decay behavior of a particular sample. There is no way to predict if any particular atom will decay at

[2] [Public domain], via Wikimedia Commons

any given moment, but the half-life is constant for a large sample of that same nuclide. The half-life is critical to know because it indicates the amount of time a sample will be emitting useful or dangerous amounts of radiation. Another way of representing the half-life is by referencing the decay constant. The decay constant for a particular nuclide is given as:

$$\lambda = \frac{\ln(2)}{\tau} \approx \frac{0.693}{\tau}$$

The decay constant has units of per time, and is often referenced instead of half-life when it is of calculational convenience.

Another important property of a radioactive sample is its activity. Activity describes the number of decays happening per unit time. Common units for activity include inverse time, Becquerels (Bq, equivalent to per second), and the Curie (Ci, equivalent to $3.7 * 10^{10}$ Bq). The Curie was chosen as a unit because it originally defined as the activity of one gram of Radium 226. Activity is modelled by exponential decay such that

$$A = A_0 e^{-\lambda t}$$

Where t is the amount of time from the initial activity. Activity is useful for determining the output of a source over time.

### 2.1.4  Interactions with Matter

Each type of radiation emission interacts with matter in different ways, since this project focuses on the interactions of electromagnetic wave emissions (x-rays and gamma rays), that is the type of matter interactions this section will focus on.

The three main types of photon interactions are the photoelectric effect, Compton scatter, and pair production. These different interactions will involve different amounts of energy absorption by the material and alteration of the photon energy and wavelength. The photoelectric effect describes the phenomena by which a photon is completely absorbed by the material and as a result, a photoelectron is ejected. The incoming photons need to have an energy greater than a threshold frequency in order to separate the electron from its orbital. If the incoming photon does not eject an electron, but is absorbed within the atom, the atom will be left in an excited state, and can emit a photon to lower its energy. This photon will have the same energy as the incoming one, but will be travelling in a different direction, this event is called coherent scattering.

Pair production occurs when a photon passing near a nucleus produces an electron and positron pair such that the momentum of the photon is conserved. This primarily happens with high energy photons because the energy of the photon must surpass the sum of the rest mass energies of the electron and positron (which adds to 1.022 MeV).

Finally, photons can scatter in an ineleastic collision with a charged particle (usually an electron), resulting in part of the photon energy to be transferred to the electron, and a change of wavelength in the photon. The wavelength change of the photon in a Compton scatter event is described by the following relation:

$$\lambda' - \lambda = \frac{h}{m_e c}(1 - \cos\theta)$$

Where $\lambda$ is the initial wavelength, $\lambda'$ is the changed wavelength of the scattered photon, and $\theta$ is the angle of the scattered photon with respect to its initial direction. Compton scatter is an important concept in radiation physics because it can obscure the measurements of radiation. This scatter is one of the main sources of error when taking measurements because photons which, along their initial direction of travel, would not have entered the detector can be scattered into them, skewing the resulting count.

Through all of these interactions, the radiation will lose its intensity as it passes through a material. This process of losing intensity is called attenuation, and is very important when dealing with shielding. The particular attenuation properties for a given setup depends on the material the radiation is passing through, the energy of that radiation, and what kind of radiation it is. In the case of this particular project, it is sufficient to note that the distance between the radiation source and the detector is enough that attenuation in air can cause non negligible error in measurements.

## 2.1.5 Measuring Radioactive Sources

Ionization chambers are commonly used to measure the output of a radioactive source. These devices, when hooked up to an electrometer, measure the amount of charge created within a sealed volume of air due to incoming ionizing radiation. The chamber is composed of a sealed chamber containing a gas (in this case air) connected to two electrodes held at a potential difference. These electrodes are attached to opposite sides of the chamber, and when a photon enters the chamber and ionizes an atom, the freed electron is drawn to the positively charged plate and the corresponding ion is drawn to the negatively charged plate. The ion pairs collide with the anode and cathode, generating a current measureable by the electrometer. A diagram of a parallel-plate ionization chamber is shown below in Figure 3.
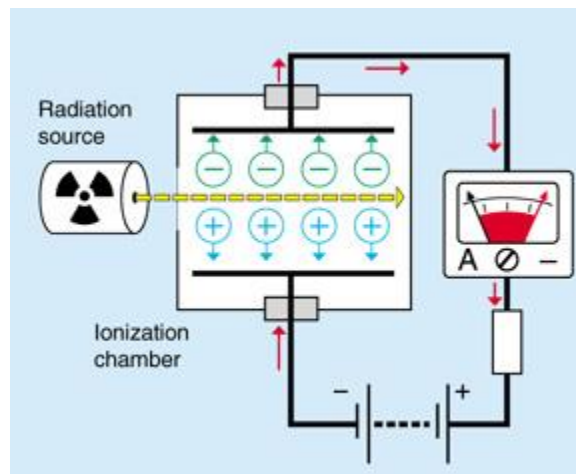


**Figure 3:** Parallel Plate Ionization Chamber[3]

One thing to consider with these ionization chambers is that is the potential difference is not strong enough, then the ions and electrons can recombine before they collide with the plates, resulting in the chamber underestimating the number and strength of ionizations

---

[3] Image from European Nuclear Society at:
https://www.euronuclear.org/info/encyclopedia/i/ionizationchamber.htm

happening. The voltage at which the potential difference is just sufficient enough to ensure all ion pairs collide with the plates is represented as $V_0$ and the current needed to produce that voltage is called the saturation current.

In order for the ionization chamber to operate properly, two more conditions need to be satisfied. First, the chamber needs to be at charged particle equilibrium (CPE). If the chamber is not at CPE, then it is possible for some ionizations to have enough energy to escape the detector and therefore not be measured. This is fortunate because for reasons discussed in section 2.5.1, CPE is also required to approximate kerma as absorbed dose. Secondly, the detector needs to receive uniform irradiation. This means that the chamber must be held at a distance from the source and not directly next to it.

## 2.2 Radiation in Biology

Radiation interacts with biological systems to cause mutagenesis or cell death. Mutagenesis occurs when a radiation interaction results in the change in the sequence of the organisms' genotype. Cell death is defined not just by the simple death of a cell, but rather by its clonogenic death, that is, when it can no longer undergo mitosis. The most efficient way to cause clonogenic cell death is by damaging the cell's DNA past the point where it can repair itself. This section deals with how radiation can cause changes within the DNA of a cell and how it can cause a biological effect.

### 2.2.1 Radiation Interactions with DNA

Radiation can produce a variety of chemical changes within DNA including nitrogenous base change, and strand breaks. The interaction between radiation and DNA occurs in two ways: direct and indirect actions. A direct action is when the radiation acts directly on the critical target, i.e. the photon interacts directly with the DNA and deposits enough energy to break the strand. Through an indirect action, the radiation interacts with a non-critical target which then interacts with the DNA to cause a biological effect. An indirect action in this case describes the process by which a photon interacts with a non DNA molecule (usually water), producing a free radical that interacts with the DNA in such a way as to cause an observable biological effect (most likely a double strand break). Figure 4 shows the difference between a direct and indirect action.
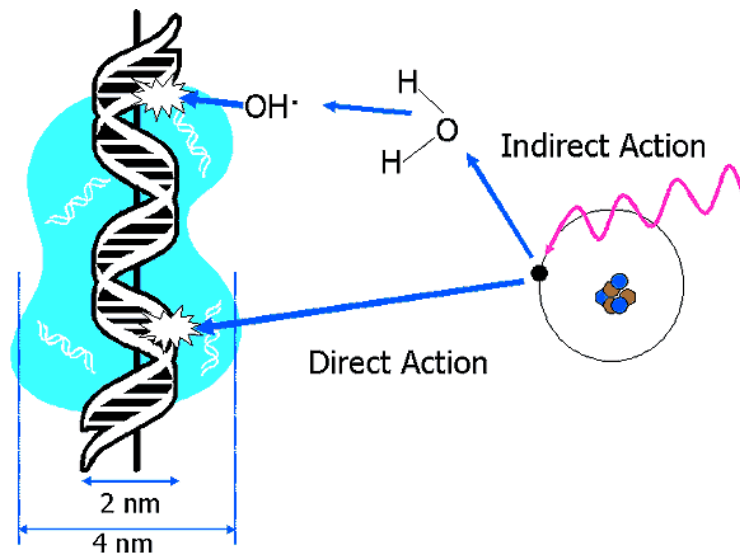
**Figure 4:** Direct vs. Indirect Action[4]

For photons, the most common way to cause DNA breakage is through indirect actions. The initial interaction between the ionizing radiation and the water molecule triggers the release of an electron and a highly reactive chemical agent known as a free radical. An orbital shell is populated by pairs of electrons which form the bonds between other atoms. When one of those electrons is removed, like from ionizing radiation, the orbital shell becomes highly unstable and seeks to replace that electron and remove the unbalance. The unpaired electron present in these molecules is called the free radical. Once the free radical is created, it diffuses in a random direction within the cell, travelling between 30-100 μm before interacting with another molecule, in this case, DNA.

The most relevant form of damage caused by radiation is a break in the sugar phosphate backbone of DNA. The ionizing radiation or free radical will interact with and break the phosphodiester bond which connects the nitrogenous bases together. When two of these breaks happen between base pairs either opposite or closely separated base pairs, it results in a double strand break and the two pieces of DNA are broken apart. Both single strand and double stranded breaks can result in cell death or carcinogenesis if unrepaired, but since cells with more than one set of chromosomes can almost always repair a single strand break, they are of little biological consequence. Double strand breaks, however, have fewer repair processes and are more likely to result in cell death.

The three outcomes of DNA damage and improper repair are apoptosis (programmed cell death), permanent dormancy (called senescence), or unregulated cell division which can lead to the formation of a cancerous tumor. For a typical mammalian cell, the average dose at which clonogenic results in half of the cell population is between 1-2 Gy[7]. At this exposure, base damage occurs at a rate of >1000 per cell, single strand breaks occur at around 1000 per cell, and double strand breaks have an incidence of around 40 per cell. Cell survival is most closely tied to double strand breakage, and single strand breaks are mostly inconsequential.

---

## 2.3  Radiation in Medicine and Cancer Therapy

Radiation is an often used tool in a hospital, whether for diagnostic imaging or for therapy treatments. One of the most ubiquitous uses of radiation in medicine is in x-ray imaging in computerized tomography (CT), which takes advantage of the different absorbance properties of matter to image internal structures of non-uniform objects (in these cases, a patients' anatomy). Other applications of radiation in medicine include PET scans and radiation therapy in cancer treatments.

Radiation therapy is a common method of treating cancers, whether through the use of external beam therapy (EBT) or through brachytherapy. EBT uses one or more beams of high energy collimated x-rays to deliver dose to the patient's tumor. This kind of treatment is noninvasive and can spare much of the surrounding tissue through careful treatment planning. EBT is used to treat many types of cancers including breast, lung, colorectal, and head and neck cancers[8]. Brachytherapy, in contrast, treats tumors from within the patient's body, and as such uses very different methods of treatment planning.

### 2.3.1  Brachytherapy

In brachytherapy, a radioactive seed is placed in or near a tumor in order to treat it. These seeds can be categorized into two types, low dose rate (LDR) and high dose rate (HDR). LDR brachytherapy uses many radioactive seeds bound together in rows that are then implanted into the treatment area. LDR brachytherapy can be used as a temporary or a permanent implant. If permanent, these seeds will emit low levels of radiation (up to weeks or even months) until they decay and harmless implant is simply left inside the patient. LDR brachytherapy is most commonly used to treat prostate cancer.

On the other hand, high dose rate (HDR) brachytherapy seeds are only temporarily kept within the patient by placing them inside a catheter or other slender tube, sliding them next to the tumor for the specified amount of time (more on the order of minutes), and then withdrawn and removed from the patient. One patient can receive HDR brachytherapy several times over the course of their treatment. These HDR seeds, rather than being in a series of rows, are often the size and shape of a grain of rice. The radioactive material is enclosed within a heavy metal casing and attached to a cable that allows it to be drawn through the catheter. The figures below illustrate the size[5] and specifications[6] of two representative HDR sources.

---

[5] Image from http://www.xoftinc.com/products_hdrsource.html

[6] Islam M A, Akramuzzaman M M, Zakaria G A. Dosimetric comparison between the microSelectron HDR [192] Ir v2 source and the BEBIG ^{60}Co source for HDR brachytherapy using the EGSnrc Monte Carlo transport code. J Med Phys 2012;37:219-25
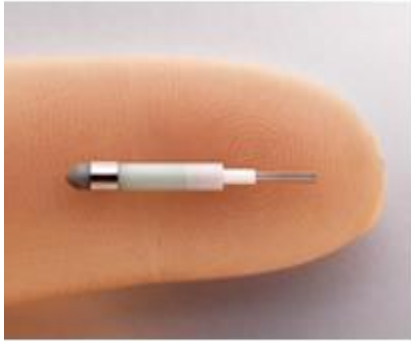
**Figure 5:** HDR source in relation to a human finger
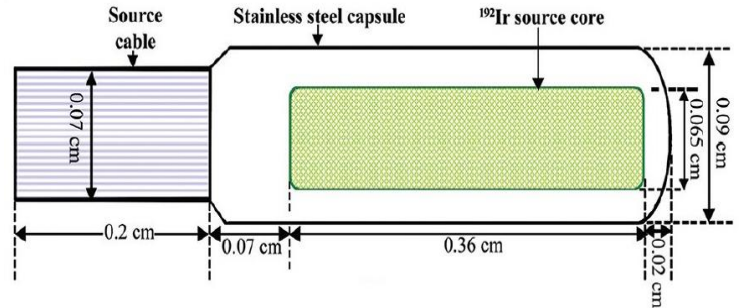
**Figure 6:** Diagram of an Ir-192 HDR brachytherapy source

Figure 6 shows a brachytherapy seed containing a core of Ir-192, a commonly used isotope for HDR brachytherapy, but there are other elements one can choose from when planning a brachytherapy treatment. The specific element chosen depends on the particular emission behavior for that source. Important factors for consideration include half-life, activity, and decay products. Half-life and activity are important for treatment planning purposes, for example calculating how long the patient should receive treatment, how much dose the patient will be receiving, and whether the source with be temporary or permanent. The decay products of the source are also of great importance because only the photon emissions are able to provide effective treatment, so if the prospective element does not emit any gamma rays, it is not a good choice for a brachytherapy source.

HDR brachytherapy can be used to treat several different cancers using varied delivery systems. In interstitial HDR brachytherapy, often used for prostate cancer, the seeds are placed directly into tissue either in or surrounding the cancer. Conversely, in intracavitary brachytherapy, used to treat breast, rectal, cervical, and vaginal cancers, the radiation is delivered to the tumor from the inside of a body cavity or into the space of a recently removed tumor.

Temporary HDR brachytherapy is a popular choice for several of these cancers, such as breast, because it localizes the dose to the cancerous tissue and spares some surrounding healthy tissue[9]. For example, for use in breast cancer treatment, brachytherapy has an advantage of EBT in that the brachytherapy treatment will spare much of the lungs that might be damaged by radiation from EBT. In addition to this, brachytherapy can be used for skin cancers by using special applicators that form to the skin to ensure the precise delivery of radiation to the cancerous tissue.

There are many different types of applicators and needles that are used to precisely place the seeds within the patient, some are made for specific applications such as the rectal/vaginal applicator shown below.

**Figure 7:** Varian brand vaginal and rectal brachytherapy applicator[7]

Each patient needs to have their treatment plan tailored for their particular circumstances. The treatment plan will dictate what type of therapy the patient will be receiving, how long and what dose they will get, where the implants will go and what type of implant they will be administered. The cancer needs to be imaged and defined as a volume within the patient. These plans are highly specialized, and require a lot of detailed information about the dimensions of the tumor and the characteristics of the seeds to be used in the brachytherapy in order to maximize the dose to the tumor and minimize the dose to the healthy tissue.

## 2.4 Source Characterization

As mentioned before, it is vitally important to understand the characteristics of a brachytherapy source before using it in clinical practice. Even after a specific type of source has been ordered, it is possible for the seeds in a given batch to have significant differences in output. Because of these discrepancies, each brachytherapy source needs to be calibrated. This section discusses the standard way to characterize sources.

### 2.4.1 Air Kerma Strength

Medical physicists use absorbed dose rate of individual HDR sources in order to design treatment plans. However, since it is very difficult to measure absorbed dose or kerma in a material, air is substituted for the material, and the value adjusted for the appropriate material. This allows physicists to use basic measurement equipment like ionization chambers to measure these quantities.

In order to understand why air kerma is used instead of absorbed dose to calibrate these sources, it is important to understand the difference between those two quantities. Absorbed dose describes the energy deposited within a mass of material due to ionizing radiation, while kerma describes the sum of the initial energies of all the charged particles created by uncharged ionizing radiation. An easy way to understand the difference between the two quantities is show in the figures below.

---

[7] Image from https://www.varian.com/oncology/products/treatment-delivery/brachytherapy-afterloaders-applicators/capri
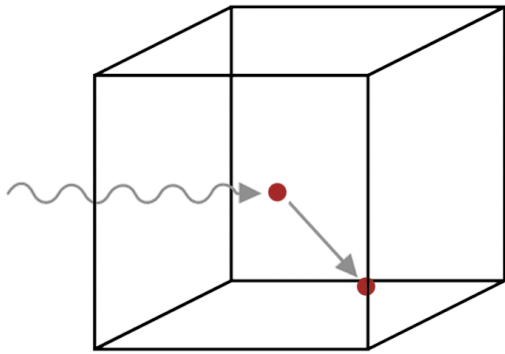
**Figure 8:** Absorbed dose, energy stays within mass       **Figure 9:** Kerma, energy can leave mass
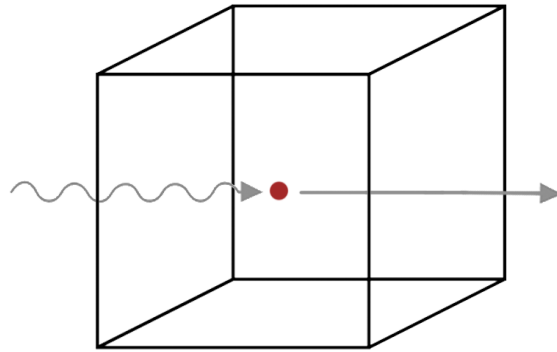
Although these two quantities are different, under particular circumstances kerma can be equivalent to absorbed dose. This is fortunate, because it is extremely difficult if not impossible to measure absorbed dose in a lab. It is very simple, however, to measure the amount of energy produced by ionizing radiation using an ionization chamber and an electrometer.

In order for absorbed dose and kerma to be equivalent, the mass taking the measurement must be thin so as to not cause significant attenuation, and the material must be under charged particle equilibrium (CPE). CPE occurs when there are an equal number of ionizing radiations leaving the material as there are entering it, this can happen due to secondary ionizing radiations being created by the initial ionizing radiation. CPE happens when the material being irradiated is thicker than the maximum penetration range of the most energetic electron which can be produced by the radiation in the material. Since CPE is satisfied by the ionization chamber volume, kerma can be used as a substitute for absorbed dose.

Once the air kerma is measured, it can be multiplied by the activity of the source to yield the air kerma rate, or the amount of energy created in a material by ionizing radiation over time. This correlates to the necessary measurement of absorbed dose rate, which is needed for treatment planning. But beyond a time dependency, there is also a distance dependency, so air kerma strength was devised. Air kerma strength is nothing more than the air kerma rate multiplied by the square of the distance from the source. This is necessary because the measurement of air kerma is taken at a large enough distance such that the oblong nature of the seed effectively reduces to a point source. However, during treatment the source will be much closer to the tumor and treated tissue.

In summary, the value given by the ionization chamber represents the air kerma strength of the source at that particular distance, and simply by dividing that value by the distance squared, the air kerma rate and subsequently the absorbed dose rate can be calculated.

### 2.5.2 The Seven-Distance Technique

The current method used to perform air kerma strength calibration tests is called the seven-distance technique created by Goetsch et. al. in 1990[4]. In this method, the source is measured in air using an ionization chamber seven different times spaced seven different distances from the source. However, this method introduces a lot of uncertainty due to the

scatter off of the air and nearby surfaces, attenuation of the photons in the air, and data regression due to fitting data to the curve provided by those seven data points.

The formula used to calculate the air kerma strength using the distance test is:

$$S_k = \frac{N_k \cdot M_p \cdot d^2}{\Delta t}$$

Where $S_k$ is the air kerma strength, $N_k$ is a calibration factor specific to each ionization detector given by the manufacturer, d is the distance, $\Delta t$ is the length of time irradiated for a given distance, and $M_p$ is the value given by the electrometer adjusted for scatter. In addition to the correction factor in M, there also needs to be a correction factor to the distance d to account for the error in measuring the center to center source-chamber distance.

The reason for taking so many measurements in the seven-distance technique is not only taking enough data points to solve for those corrections, but also enough to average several different solutions together to increase accuracy.[4]

## 2.5    Monte Carlo Simulations – MCNP

Before a physical single measurement system can be built. It needs to first be optimized to produce the least amount of error. To this end it is possible to simulate multiple different configurations of a potential single measurement geometry using specialized software running a Monte Carlo simulation. This section discusses what a Monte Carlo simulation is and some qualities of the particular software used in this project.

A Monte Carlo method is a computational tool used to repeatedly simulate a random event for the purpose of obtaining numerical data. In this case, the random event being simulated is the emission of a radiation from a particular isotope. By accurately describing the conditions of the single measurement geometry and the emission energies and probabilities, the Monte Carlo program can, over numerous repetitions, construct the overall average behavior of that system.

The particular program being used in this project is called Monte Carlo N-Particle code, or MCNP. MCNP is specifically designed to simulate radiation events, and is built to provide flexibility in source definition, environment construction, and data collection. MCNP was created by the Los Alamos National Laboratory[10] for use in simulating neutron, photon, electron, or coupled transport. For the purposes of this particular project, only the photon simulating capabilities will be accessed.

MCNP code is structured into distinct cards, each of which corresponds to a different part of the system it is simulating or to the specifications of the data collection. There are separate cards used for defining the surfaces, volumes, sources, materials, and data tallies. The surface card is used to construct the skeleton of the geometry. For example, if a hollow sphere needs to be constructed, the surface card will contain two lines for two spheres, one defining the interior surface of the shell and one defining the exterior surface of the shell. The cell card of MCNP defines the volumes in relation to the surfaces, and also the density of the material within each volume. Continuing the previous example, the cell card would be responsible for defining the shell of the sphere as being all space contained inside of the exterior sphere surface and outside the interior sphere surface, as well as the density of the material within that space.

The next cards define the source and materials needed to construct the geometry. The source card in the code for this project contains a simple point source located at the origin, so the vast majority of this card was simply defining the energies of all potential emissions and the corresponding probabilities of those emissions. The materials card is simple as well, it contains a description of every material being assigned to a cell in the geometry based on the molecular composition of that material.

The last few things that need to be defined are the particles which will be simulated, the number of repetitions of the simulation, and which data tallies will be used. For this project, only the photons needed to be simulated, and the number of cycles is large enough such that the stochastic error of the program decreased to an acceptable number (between 1-2%). Finally, the data tally represents the values and data collection that MCNP will take when it runs the code. In this case, the tally mode will output the average energy deposited in a given cell in units of MeV/g.

# 3    Methods

Before the coding began to test all the of the different geometries, it was important to first consider the following factors: potential scatter off of the wall material, stochastic error from MCNP, and constructible practicality. This section will discuss the methodology of creating the simulations including design and coding considerations.

## 3.1    Experimental Design

Overall the entire geometry for the system is represented by a giant sphere representing the end of the world, past which all emission information can be discounted, two boxes representing the inner and outer topography of the walls, a source defined at the origin, and a sphere $0.64\ cm^2$ in volume simulating the ionization chamber detector volume placed 10 cm from the origin along the x axis. The materials defined were air inside the detector sphere and outside the cube, a vacuum inside the box but outside the sphere, and either aluminum, lead, or steel between the two wall surfaces. Aluminum, lead, and steel were all chosen for their common use in shielding and commercial availability.

The three isotopes simulated were Iodine 125, Iridium 192, and Ytterbium 169. These three isotopes span a range of energy outputs, and will serve to ensure that the geometry is optimized for more than a single isotope. Iodine and Iridium were chosen because they are commonly used in brachytherapy sources available for clinical use. Ytterbium was chosen because it is of potential research interest for development of a new type of brachytherapy seed.

The vacuum within the box will negate any potential error in the measurement due to attenuation in the space between the source and the detector. Additionally, the 10 cm distance between the source and the sphere of air will give enough space such that the detector will receive uniform irradiation. Figure 10 illustrates the general geometry being simulated.
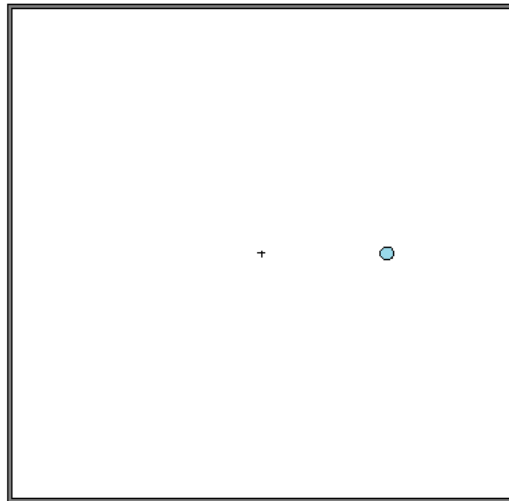


**Figure 10:** General Geometry of Single Measurement Air Kerma

### 3.1.1  Wall Characteristics

The three chosen wall materials to test were aluminum, lead, and steel. Since the material definition requires the input of the amount of individual elements present, a specific alloy needed to be chosen. For these experiments, steel alloy 304 was chose as it is a commonly used alloy. The wall thicknesses used were 1/4" for the aluminum walls and 1/8" for the lead and steel walls. In addition to varying the wall material, the size of the cube was also varied. The initial geometry setup put the length of the walls at 40 cm. Further tests simulated two larger sized cubes, with wall lengths of 60cm and 90cm respectively. In addition to these simulations, another geometry was run where there was no box, it was simply source and detector in a vacuum. This test was done in order to obtain the "true" measurement of dose deposition such that any additional dose counted in the walled geometries could be attributed to scatter.

The first cube size that was simulated was the smallest, 40 cm. This number was chosen as a base from which we could estimate the feasibility of the system, and how much larger or smaller the box could be and still have minimal error. The results from these measurements drove the test of the 60 cm box. This yielded a significant decrease in error, so a final test was done at 90 cm to see if the error would continue to decrease in a similar manner or if it had bottomed out.

### 3.1.2  Source Characteristics

The sources were defined in the MCNP program by the energy of their emissions and the probability of each of those emissions. Using the data provided by The Lund/LBNL Nuclear Data Search[11], the emissions of each of the radioisotopes were transferred and ordered into the code in increasing order of energy. All photon emissions occurring with a probability of greater than 0.001% were used to ensure the most accurate simulation possible.

## 3.2  Coding

The code was programmed such that the output of the program was the average energy deposited in the sphere of air for a single radiation event. As more events were simulated, the value given becomes more and more true to the actual behavior of the radioisotope. One thing to note, is that the probability of the emissions do not necessarily add up to exactly 100%. In fact, all of the radioisotopes simulated had total emission probabilities of greater than 100%. This effectively means that one radiation event can result in more than one emission. In order to correct for this effect in the program, the energy deposition given from the program was multiplied by the added probability of any emissions for a particular source.

Examples of working code exhibiting each manipulated aspect are included in the appendices.

After each of the programs were run and energy deposition adjusted, they were all stored in an excel file along with the error given by the program representing the stochastic uncertainty inherent in Monte Carlo simulations. This error is due to the random process of choosing a particular event to simulate, and can be lowered by increasing the number of simulations run for a particular geometry. To this end, 20 million radiation events were simulated for any given geometry, lowering the error to an acceptable range of 1.02-2.66%.

# 4    Results

This section will present the data obtained from all of the simulations in all iterations of the single measurement geometry. The data gathered from each simulation were the average energy deposited in the sphere volume for a single radiation event in MeV/g and the error given by MCNP in that measurement. These measurements were adjusted as described above for their respective isotope and then compiled into three tables for each size cube. Below is the table produced for the 60 cm walled cube, the tables for the other two cube sizes are included in the appendices.

**Table 1: Energy Deposition and Error for 60 cm cube**

|            | Iodine | | Iridium | | Ytterbium | |
|------------|-----------|-----------|-------------|---------|-------------|---------|
|            | MeV/g     | Error (%) | MeV/g       | Error % | MeV/g       | Error % |
| No wall    | 3.80E-05  | 2.58      | 2.08E-05    | 1.03    | 3.72E-05    | 2.08    |
| Aluminum   | 3.83E-05  | 2.66      | 2.09E-05    | 1.02    | 3.73E-05    | 2.07    |
| Steel (304)| 3.83E-05  | 2.62      | 2.08521E-05 | 1.03    | 3.7901E-05  | 2.08    |
| Lead       | 3.82086E-05| 2.62     | 2.08478E-05 | 1.03    | 3.72899E-05 | 2.07    |

In this table, the measurement from the geometry containing no wall represents the true energy deposition, so by comparing that value against the energy deposition obtained in the walled geometries, the error to due scatter was calculated. In order to better visualize this data, the following charts are provided for Iodine as a representative of the other charts (included in the appendices).
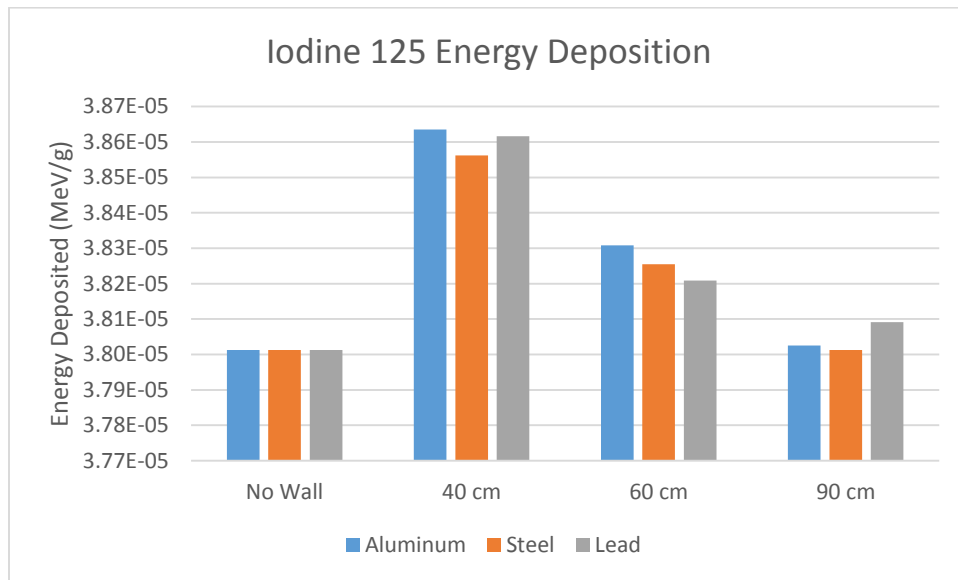


**Figure 11:** Energy Deposition from an Iodine 125 Source
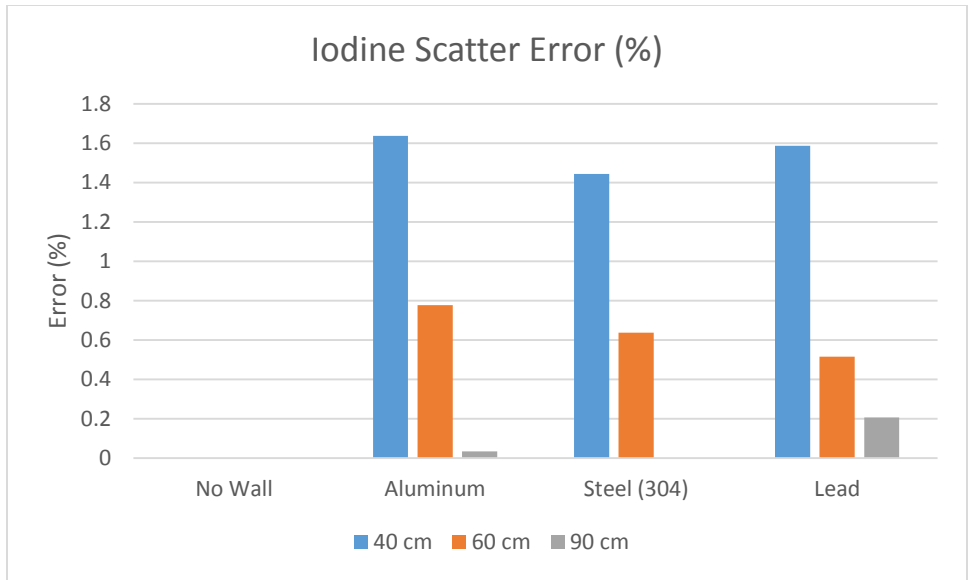
**Figure 12:** Scatter Error from an Iodine 125 Source

In addition to this, the total error of the system had to be examined. There is the error from the stochastic nature of the Monte Carlo method, specific to each simulation, and then an approximate 1% uncertainty due to MCNP photon cross section error. For each simulation the three sources of error were added in quadrature to calculate the total error for each measurement from MCNP. Again, the total error for the Iodine source is given as an example below, the other two are in the appendices.
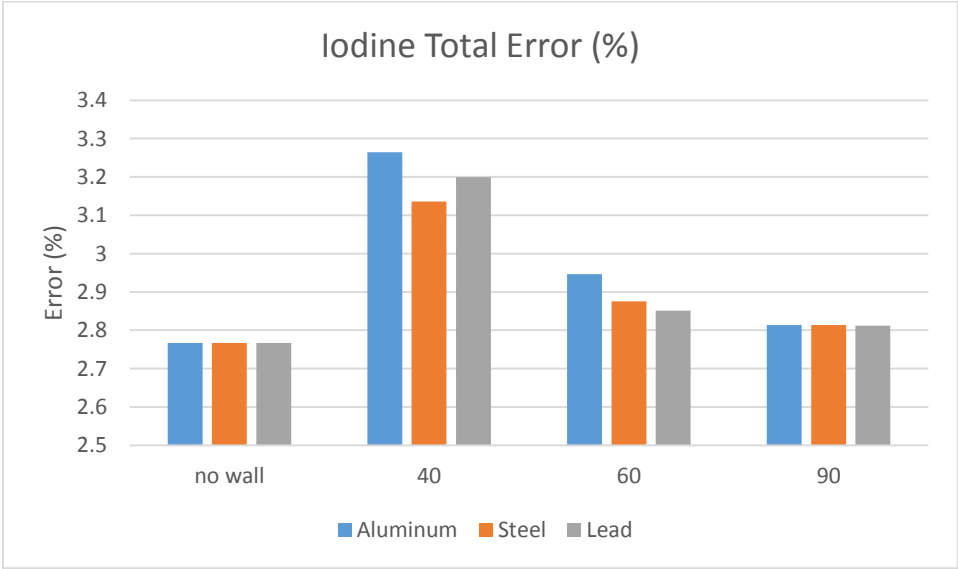


**Figure 13:** Total Uncertainty in Iodine 125 Measurements

# 5    Conclusions

Based on the data obtained from the MCNP simulations, an optimized design that best fits the practical needs of the lab can be chosen. Furthermore, the data shows that using an optimized design reduces the error to less than the estimate 3-4% of the seven-distance technique[5]. Adding that in to the fact that the single measurement procedure would be much easier to conduct, and it is clear that this system is not only feasible, but preferable to the current seven-distance method.

## 5.1    Optimized Design

The 90 cm box offered lower amounts of error across all isotopes and mall materials, however when compared against the 60 cm results the difference is not large enough to justify the significantly larger space it would take in a lab. As far as wall materials go, lead produces the best shielding across the range of isotopes, however its structural properties make it a poor wall choice if it is the only material present in the wall. Therefore, a wall material of steel or a combination of both steel and lead is recommended unless testing of further wall materials produces a better result.

Construction of this design would allow the university to measure HDR brachytherapy sources for research purposes in house. Specifically, this will allow for research developing new or studying existing seed types and treatment planning options. Of most immediate interest is the possibility of Ytterbium 169 as a potential brachytherapy source, which is not well researched in terms of dosimetric and medical applications. The radiation laboratory can begin to pursue these research avenues with higher accuracy and ease because of this apparatus.

## 5.2    Future Suggestions

Based on these results, further exploration into different wall materials such as glass or forms of plastic should be considered. Furthermore, the shape of the geometry can be changed in order to further minimize scatter. For example, the shape of the container could be changed to a cylinder rather than a cube. If desired, one could also shift the position of the source and sphere within the structure such that the source is not precisely on the origin, but rather moved along an axis or xyz plane.

# References

[1] Howlader N, Noone AM, Krapcho M, Garshell J, Miller D, Altekruse SF, Kosary CL, Yu M, Ruhl J, Tatalovich Z,Mariotto A, Lewis DR, Chen HS, Feuer EJ, Cronin KA (eds). SEER Cancer Statistics Review, 1975-2012, National Cancer Institute. Bethesda, MD, http://seer.cancer.gov/csr/1975_2012/, based on November 2014 SEER data submission, posted to the SEER web site, April 2015

[2] "Leading Causes of Death." *Centers for Disease Control and Prevention.* Centers for Disease Control and Prevention, 25 Feb. 2016. Web. 02 Apr. 2016.

[3] L. A. DeWerd. Calibration for brachytherapy sources, 2005. URL www.aapm.org/meetings/05SS/program/dewerd_sumsch.pdf. University of Wisconsin.

[4] S. J. Goetsch, F. H. Attix, D. W. Pearson, and B. R. Thomadsen. Calibration of 192-ir high-dose-rate afterloading systems. Technical report, University of Wisconsin Medical School, 1990.

[5] D. C. Medich. Direct measurement of yb-169 air kerma strength by photon spectroscopy. University of Massachusetts Lowell, 2008.

[6] E. J. Hall. Radiobiology for the Radiologist. Lippincott Williams & Wilkins, Philadelphia, PA, 6th edition, 2005.

[7] Beaulieu Danielle. Air Kerma Strength Measurement of a Cs-137 Radioisotope Using a Seven-Distance Ionization Technique and Comparison with the Gamma Spectroscopy Method. Worcester Polytechnic Institute, 2013.

[8] RSNA. External beam therapy (ebt), 2013.

[9] R. Stanton and D. Stinson. Applied Physics for Radiation Oncology. Medical Physics Publishing, Madison, WI, 1996.

[10] Monte Carlo Code Group. Los Alamos National Laboratory. https://mcnp.lanl.gov/

[11] Periodic Chart Interface to the Nuclides. The Lund/LBNL Nuclear Data Search. http://nucleardata.nuclear.lu.se/toi/perchart.htm

# Appendix A: MCNP Code

## Code for Iodine 125 Source, Aluminum Walls, 40 cm Length

```
c
c Cell cards
c
10 1 -0.001225  (-1)   imp:p,e=1 $ sphere
20 0           (-2 1) imp:p,e=1 $ inside wall outside sphere
30 2 -2.7      (-3 2) imp:p,e=1 $ wall thickness
40 0           (3 -4) imp:p,e=1 $ outside wall
50 0           (4)    imp:p,e=0 $ end of the world

c
c Surface cards
c
1 sx 10 0.5346      $ sphere
2 BOX -20 -20 -20 40 0 0 0 40 0 0 0 40   $ box
3 BOX -20.635 -20.635 -20.635 41.27 0 0 0 41.27 0 0 0 41.27
4 so 500           $ end of the world

c data cards
mode p
c
c f6 tally for deposited dose in sphere (MeV/g/simulated photon)
F06:p    10
c
c end tally section
c
c
c Source is a point source of I-125 at origin
SDEF Par 2 pos 0 0 0 erg d1
SI1 L 0.0033 0.0036 0.0038 0.0038 0.0040 0.0041 0.0041 0.0042
      0.0043 0.0046 0.0048 0.0048 0.0269 0.0272 0.0275 0.0309
      0.0310 0.0312 0.0317 0.0318 0.0355
SP1   0.0023 0.0011 0.0063 0.0560 0.0350 0.0042 0.0070 0.0004
      0.0101 0.0045 0.0010 0.0016 .00003 0.4060 0.7570 0.0683
      0.1320 0.0012 0.0381 0.0058 0.0668
c end source term definitions
c
c Define the material(s) present in the model
c m1 is air, m2 is aluminum
m1 6000 -0.00012 7000 -0.75527 8000 -0.23178 18000 -0.01283 GAS=1        $ Air
m2 13000 1     $ Aluminum wall material
c
c end material definitions
c
nps 20000000
```

```
c
c Cell cards
c
10 1 -0.001225  (-1)   imp:p,e=1 $ sphere
20 0        (-2 1) imp:p,e=1 $ inside wall outside sphere
30 2 -2.7     (-3 2) imp:p,e=1 $ wall thickness
40 0        (3 -4) imp:p,e=1 $ outside wall
50 0        (4)   imp:p,e=0 $ end of the world


c
c Surface cards
c
1 sx 10 0.5346      $ sphere
2 BOX -30 -30 -30 60 0 0 0 60 0 0 0 60   $ box
3 BOX -30.3175 -30.3175 -30.3175 60.635 0 0 0 60.635 0
    0 0 60.635
4 so 500          $ end of the world

c data cards
mode p
c
c f6 tally for deposited dose in sphere (MeV/g/simulated photon)
F06:p    10
c
c end tally section
c
c
c Source is a point source of Ir-192 at origin
SDEF Par 2 pos 0 0 0 erg d1
SI1 L 0.0078 0.0083 0.0088 0.0089 0.0093 0.0094 0.0100 0.0102
    0.0104 0.0105 0.0106 0.0108 0.0109 0.0111 0.0112 0.0116
    0.0121 0.0124 0.0125 0.0129 0.0133 0.0134 0.0609 0.0615
    0.0630 0.0645 0.0651 0.0668 0.0711 0.0714 0.0719 0.0734
    0.0736 0.0754 0.0757 0.0762 0.0778 0.0781 0.1101 0.1363
    0.1770 0.2013 0.2058 0.2800 0.2833 0.2960 0.3085 0.3165
    0.3293 0.3745 0.4165 0.4205 0.4681 0.4846 0.4853 0.4890
    0.5886 0.5934 0.5994 0.6044 0.6125 0.7040 0.7658 0.8845
    1.0615 1.0897 1.3783
SP1   0.0003 0.0008 0.0006 0.0057 .00009 0.0164 0.0003 0.0005
    0.0041 0.0006 0.0013 0.0002 0.0007 0.0124 0.0042 0.0003
    0.0008 0.0002 0.0002 0.0025 0.0005 0.0003 .00001 0.0120
    0.0207 .00003 0.0265 0.0453 0.0024 0.0046 0.0001 0.0016
    0.0002 0.0053 0.0103 0.0003 0.0037 0.0005 0.0001 0.0018
    0.0043 0.0047 0.0330 0.0002 0.0026 0.2867 0.3000 0.8281
    0.0002 0.0072 0.0066 0.0007 0.4783 0.0318 .00002 0.0044
```

```
     0.0452 0.0004 .00004 0.0823 0.0531 .00005 .00001 0.0029
     0.0005 .00001 .00001
c end source term definitions
c
c Define the material(s) present in the model (m1 air m2 steel)
m1 6000 -0.00012 7000 -0.75527 8000 -0.23178 18000 -0.01283 GAS=1
m2 6000 -0.00080 24000 -0.1900 25000 -0.0200 28000 -0.09000
     15000 -0.00045 16000 -0.0003 14000 -0.001 26000 -0.69745
c
c end material definitions
c
nps 20000000
```

## Code for Ytterbium 169 Source, Lead Walls, 90 cm Length

```
c
c Cell cards
c
10 1 -0.001225  (-1)   imp:p,e=1 $ sphere
20 0         (-2 1) imp:p,e=1 $ inside wall outside sphere
30 2 -11.342    (-3 2) imp:p,e=1 $ wall thickness
40 0         (3 -4) imp:p,e=1 $ outside wall
50 0         (4)    imp:p,e=0 $ end of the world


c
c Surface cards
c
1 sx 10 0.5346      $ sphere
2 BOX -45 -45 -45 90 0 0 0 90 0 0 0 90   $ box
3 BOX -45.3175 -45.3175 -45.3475 90.635 0 0 0 90.635 0
     0 0 90.635
4 so 500           $ end of the world

c data cards
mode p
c
c f6 tally for deposited dose in sphere (MeV/g/simulated photon)
F06:p    10
c
c end tally section
c
c
c Source is a point source of Yb-169 at origin
SDEF Par 2 pos 0 0 0 erg d1
SI1 L 0.0063 0.0071 0.0072 0.0073 0.0080 0.0081 0.0082 0.0084
     0.0085 0.0094 0.0097 0.0098 0.0208 0.0428 0.0493 0.0498
```

```
        0.0507 0.0515 0.0573 0.0575 0.0579 0.0590 0.0592 0.0631
        0.0659 0.0720 0.0851 0.0936 0.0980 0.1014 0.1052 0.1098
        0.1140 0.1174 0.1182 0.1305 0.1567 0.1772 0.1932 0.1980
        0.2060 0.2139 0.2403 0.2611 0.2912 0.3016 0.3077 0.3340
        0.3366 0.3709 0.3793 0.4944 0.5151 0.5799 0.6249
SP1   0.0081 0.0205 0.1850 0.0027 0.0132 0.1270 0.0221 0.0033
        0.0364 0.0228 0.0041 0.0060 0.0019 0.0025 0.0003 0.5320
        0.9400 0.0002 0.0993 0.1920 0.0038 0.0647 0.0172 0.4420
        0.0001 .00004 .00003 0.0261 .00002 .00007 .00003 0.1747
        .00009 0.0004 0.0187 0.1131 0.0001 0.2216 .00007 0.3580
        .00004 .00003 0.0011 0.0172 .00004 .00005 0.1005 .00002
        .00009 .00007 .00001 .00001 .00004 .00002 .00005
c end source term definitions
c
c Define the material(s) present in the model
c m1 is air, m2 is lead
m1 6000 -0.00012 7000 -0.75527 8000 -0.23178 18000 -0.01283 GAS=1
m2 82000 1     $ lead wall material
c
c end material definitions
c
nps 20000000
```

# Appendix B: Energy Deposition Tables

### Energy Deposition for 60 cm Box

|  | Iodine | | Iridium | | Ytterbium | |
| --- | --- | --- | --- | --- | --- | --- |
|  | MeV/g | Error (%) | MeV/g | Error % | MeV/g | Error % |
| No wall | 3.80E-05 | 2.58 | 2.08E-05 | 1.03 | 3.72E-05 | 2.08 |
| Aluminum | 3.83E-05 | 2.66 | 2.09E-05 | 1.02 | 3.73E-05 | 2.07 |
| Steel (304) | 3.83E-05 | 2.62 | 2.09E-05 | 1.03 | 3.79E-05 | 2.08 |
| Lead | 3.8209E-05 | 2.62 | 2.085E-05 | 1.03 | 3.729E-05 | 2.07 |

### Energy Deposition for 90 cm Box

|  | Iodine | | Iridium | | Ytterbium | |
| --- | --- | --- | --- | --- | --- | --- |
|  | MeV/g | Error (%) | MeV/g | Error % | MeV/g | Error % |
| No wall | 3.80E-05 | 2.58 | 2.08E-05 | 1.03 | 3.72E-05 | 2.08 |
| Aluminum | 3.80E-05 | 2.63 | 2.09E-05 | 1.03 | 3.72E-05 | 2.08 |
| Steel (304) | 3.8013E-05 | 2.63 | 2.085E-05 | 1.03 | 3.763E-05 | 2.08 |
| Lead | 3.8091E-05 | 2.62 | 2.083E-05 | 1.03 | 3.72E-05 | 2.08 |

# Appendix C: Energy Deposition and Scatter Charts



Ytterbium 169 Energy Deposition



Iridium 192 Energy Deposition

Ytterbium Scatter Error (%)



Iridium Scatter Error (%)

Ytterbium Total Error (%)



Iridium Total Error (%)